

# Analysis of the impact of different blast energies on rock crushing using numerical modelling

Rudarsko-geološko-naftni zbornik  
(The Mining-Geology-Petroleum Engineering Bulletin)  
UDC: 622.2  
DOI: 10.17794/rgn.2025.2.7

Preliminary communication



Seyed Mohammad Reza Sahlabadi<sup>1</sup>; Kaveh Ahangari<sup>2\*</sup>; Mosleh Eftekhari<sup>3</sup>

<sup>1</sup> Department of Mining Engineering, Science and Research Branch, Islamic Azad University, Tehran, Iran, <http://orcid.org/0000-0003-3912-1291>

<sup>2</sup> Department of Mining Engineering, Science and Research Branch, Islamic Azad University, Tehran, Iran, <http://orcid.org/0000-0001-9462-7303>

<sup>3</sup> Department of Mining Engineering, Tarbiat Modares University, Tehran, Iran, <http://orcid.org/0000-0002-3126-9024>

## Abstract

The propagation of waves generated by an explosion induces both tensile and compressive stresses in the rock, impacting its mechanical and dynamic behaviour and ultimately leading to failure. Within this process, the phenomenon of crack expansion is of significant importance and has garnered the attention of various researchers in recent years. Predicting fracture geometry in rock materials, particularly in the context of crack growth, is a complex problem often necessitating advanced techniques. In this study, a blast hole was drilled into a concrete sample, and four explosion modes were examined using the discrete element method. These modes included the simultaneous modelling of shock energy, reflection, and gas pressure; the simultaneous modelling of shock energy and gas pressure; the simultaneous modelling of shock energy and reflection; and the modelling of shock energy alone. While the homogeneity observed in artificial samples like concrete may not precisely mimic that of stone samples, the findings of such research remain valuable within their limitations. The results indicate that the highest joint density, or, in other words, the most substantial rock fragmentation, occurs when all three types of shock energy, reflection, and gas pressure are present simultaneously. Furthermore, the results show that the model incorporating both gas pressure and shock energy exhibits the most significant rock fragmentation, followed by the model considering only shock and reflection energy. Finally, the model modelling shock energy alone demonstrates the least fragmentation.

## Keywords:

blast wave; shock energy; reflection energy; gas pressure; numerical modelling

## 1. Introduction

The process of drilling and using explosives is crucial in both open pit and underground mining, as well as civil construction projects like road excavation, underground spaces, tunnels, and shafts. In open pit mining, a method called bench blasting is commonly employed, involving the drilling of rows of blast holes parallel to the vertical or inclined rock face. This approach is also applicable in large-area tunnel construction, where the upper part of the tunnel is initially created as a drift, and the lower part is excavated through benching using vertical, inclined, or horizontal holes (Rustan, 1998). During the blasting operation, the explosive within the borehole undergoes a rapid chemical reaction, transforming it from a compact material into a high-pressure, high-temperature gaseous substance (Fourney, 1993; Bhandari, 1997). This transformation rate is known as the velocity of detonation (VOD), and the resulting pressure is referred to as

the detonation pressure (Ayala Carcedo and Lopez Jimeno, 1995). The equilibrium pressure of the explosion gas is directly linked to the detonation pressure, and it is typically considered to be half of the detonation pressure (Katter and Fairhurst, 1971; Ning et al., 2011). The intense stress wave, or shockwave, that affects the borehole wall is directly proportional to this latter pressure and is influenced by factors like the coupling ratio (the ratio of explosive diameter to borehole diameter), the material used for coupling, and the properties of the surrounding rock (Chi et al., 2019).

The field of rock blasting continues to hold significant relevance and intrigue within the domains of civil and mining engineering. Notably, the numerical simulation of rock blasting has garnered substantial attention, serving as a valuable complement to experimental research efforts. Potyondy et al. (1996) employed a computational methodology for simulating explosive rock breakage that integrates the separate and combined effects of shock- and gas-induced damage within a three-dimensional framework using the PFC3D discrete-element code. The rock mass is modelled as a dense assembly of

\* Corresponding author: Kaveh Ahangari  
e-mail address: [kaveh.ahangari@gmail.com](mailto:kaveh.ahangari@gmail.com)

bonded spherical particles, allowing dynamic stress waves to propagate through the structure and enabling unlimited displacement or separation under applied forces. A gas-filled discrete fracture network, represented as interconnected penny-shaped crack reservoirs at broken bond locations, is explicitly modelled. This fully coupled approach dynamically evolves fracture patterns, gas flow, and pressure distributions, providing a realistic representation of both mechanical and fluid responses in rock fragmentation. The model effectively captures the interaction between shock waves and gas pressures, offering detailed insight into crack initiation and propagation, which is critical for optimizing blasting designs in engineering applications. **Minchinton and Lynch (1996)** utilized the combined finite element-discrete element program MBM2D to model rock fragmentation and heaving during the blasting process. This study provides experimental evidence showing that a significant portion of crack development, fragmentation, and heave during blasting is driven by the high-pressure gases produced in the blast hole. Cracking in the model is restricted to tensile failure (Rankine criterion), which is influenced by both stress fields and gas flow. The latter is modelled by coupling the discrete element porosity field with a finite volume gas flow model. Simulations reveal notable qualitative differences in blasting performance between scenarios with stemming (which retains gases in the blast holes) and without stemming, underscoring the critical role of gas containment in influencing rock fragmentation. **Wang et al. (2008)** developed a centered finite difference method using a cross-format approach to study spalling in a rock plate caused by an explosive event. They then compared their results with simulations performed using LS-DYNA. The study begins by simplifying a large-scale contact explosion into a one-dimensional (1-D) strain problem, utilizing a cross-format centered finite-difference scheme. The finite-difference code is then employed to examine wave propagation in a rock plate and is compared with the commercial software LS-DYNA. Furthermore, a continuum damage model for rock is introduced and successfully integrated into LS-DYNA via a user-defined subroutine. This, combined with the erosion technique, is used to simulate blast-induced spalling damage on the backside of a rock plate. The results demonstrate that the 1-D finite difference code is both efficient and accurate, while the subroutine effectively models the spalling damage process. **Zhu et al. (2007)** investigated the dynamic fracture mechanisms associated with blast-induced borehole breakdown and crack propagation using circular rock models with a centrally placed explosive charge. The models are analyzed using the AUTODYN 2D code, incorporating four equations of state (linear, shock, compaction, and ideal gas) based on material properties and loading conditions. A modified principal stress failure criterion is applied to assess material behaviour. Dynamic stresses at selected points are calculated over time fol-

lowing the explosive load. The results reveal that shear stress, resulting from intense compressive stress, creates a crushed zone near the borehole, while the major tensile stress generates radial cracks. Reflected stress waves from the free boundary induce circumferential cracks further from the boundary. The study also explores the effects of boundary conditions, coupling media, borehole diameter, decoupling, and joint presence on rock dynamic fracture. **Wei et al. (2009)** conducted a parametric study using the transient dynamic finite element program ANSYS-LSDYNA, and the model is validated against field blast test data. This paper addresses the prediction of rock mass damage due to underground explosions, such as those caused by accidental blasts, rock bursts, or weapon attacks, which is crucial for rock engineering. Parametric studies are conducted to assess the effects of loading density, rock mass rating (RMR), and charge weight on rock mass damage induced by these explosions. A fully coupled numerical analysis, incorporating the explosion process, is carried out, with the large deformation zone near the charge solved using the Arbitrary Lagrange–Euler (ALE) method. The deformable modulus and compressive strength of granite rock mass are estimated using the RMR system. The study adopts the peak particle velocity (PPV) damage criterion and the plastic strain criterion to evaluate the damage zone around the charge hole. An empirical formula is derived from the numerical results to estimate the damage zone in granite, considering the effects of loading density, RMR, and charge weight. **Onederra et al. (2013)** introduced the Hybrid Stress Blasting Model (HSBM), a recent advancement in blasting engineering modelling. HSBM includes a rock breakage engine that simulates detonation, wave propagation, rock fragmentation, and muck pile formation. The model's accuracy is evaluated through two controlled blasting experiments. The results show that HSBM effectively predicts both the extent and shape of the damage zone, taking into account factors like the point of initiation and free-face boundary conditions. Radial fractures, extending towards the free face, were observed in the model outputs and aligned with experimental data. In the second validation experiment, the model predicted the maximum visible damage to be about 1.45 meters for a fully coupled 38-mm emulsion charge, with a minimal relative error (1.59%) for radial velocities near the charge. However, discrepancies were noted at further distances from the charge, where the model overestimated particle velocities, leading to an overestimation of the damage zone due to excessive stress reflections. Despite this, the model accurately predicted damage in the immediate vicinity of the blast hole. **Table 1** presents some numerical studies conducted in the field of rock blasting.

Initially, as the shock wave applies pressure to the borehole wall, compressive forces in all three cylindrical coordinates lead to the formation of shear bands once the rock's dynamic compressive strength is exceeded. These

**Table 1:** Some numerical studies conducted in the field of rock blasting

Researcher	Technique	Description
Trigueros et al. (2017)	Experimental investigation, previously presented equations, seismic equations	Improvement of peak particle velocity (PPV) equation
Soltys et al. (2017)	Automating the blast damage investigation process using experimental data and predetermined numerical relationships	Providing a system for recording explosive vibrations and its pathology automatically
Liu et al. (2018)	Continuous method (finite element)	Matching the obtained results with experimental data based on numerical modelling
Luccioni et al. (2018)	Lagrangian method and continuous RHT model	Matching the obtained results with experimental data based on numerical modelling
Zarate et al. (2018)	Using two finite element and discrete element methods	Matching the obtained results with experimental data based on numerical modelling
Lak et al. (2019)	Discontinuous method (discrete element)	Matching the obtained results with experimental data based on numerical modelling
Wang et al. (2023)	ALE-FEM-SPH coupling method	Numerical prediction of blast fragmentation of reinforced concrete slab
Salamy and Hammoud (2023)	Numerical modelling	Simulation of blast-induced rock tunnel damage

bands can pulverize the rock, creating a crushed zone whose size depends on detonation pressure and explosive charge coupling. As the shock wave moves away from the borehole, it transitions to tensile stress, potentially causing new radial cracks or extending existing flaws. Interaction between explosion gas and crack surfaces further propagates these cracks. The expelled gas also displaces fragmented rock, forming a muck pile, eventually reducing gas pressure to atmospheric levels (Roy, 2005; Yang et al., 2018).

Explosion mechanisms are critical for advancing practical blasting engineering. However, conducting experimental blasting studies is often prohibitively expensive, highly complex, and inherently hazardous. This underscores the necessity of developing reliable and scientifically robust numerical methods to simulate the blasting process. In geotechnical engineering, numerical modelling of blasting mechanisms has proven invaluable in assessing the effects of stress wave propagation on rock slope stability (Yan et al., 2016), optimizing tunnel excavation processes (Motoyama et al., 2014), and analyzing the dynamic response of tunnel linings under explosive loads (Tiwari et al., 2016). A comprehensive understanding of these mechanisms not only enhances the safety and efficiency of blasting operations but also facilitates the design of cost-effective and scientifically informed engineering solutions (Yang et al., 2013; Yang et al., 2019).

Despite significant advancements in numerical modelling of rock blasting, existing studies have primarily focused on the effects of shock waves and reflected energies. However, gas pressure, which plays a critical role in rock fragmentation, has often been overlooked or oversimplified in simulation studies. This omission has resulted in models that lack the ability to fully capture

the complex interactions between explosive forces and rock mechanics.

This study aims to address this gap by introducing a novel function within the PFC 2D framework to explicitly model gas pressure within fractures. By dynamically applying gas pressure perpendicular to crack surfaces as they propagate, our approach provides an unprecedented level of detail and accuracy in simulating the blast-induced fracture process. Furthermore, the study aims to analyze how explosive material characteristics affect crack development, influencing blast performance and rock crushing. Using numerical simulation (PFC 2D), the research investigates explosion behaviour and its impact on crack growth and rock crushing. Such advancements not only bridge the gap between numerical and experimental studies but also pave the way for optimizing blasting designs in mining and civil engineering applications. The simulation explores how the explosive force interacts with the rock, affecting fracture patterns and subsequent rock fragmentation, offering insight into optimizing blasting operations for various applications.

## 2. Methodology

### 2.1. Test set-up and calibration

The simulated sample is a concrete sample prepared in the laboratory and then simulated based on its rock mechanical properties (see Table 2). The mechanical tests on the concrete samples were conducted following standard procedures recommended by the International Society for Rock Mechanics (ISRM) (Ulusay, 2014). For the uniaxial compressive strength, the ISRM-suggested method for “Determination of Uniaxial Compressive Strength of Rock Materials” was followed. Cylindrical concrete samples with dimensions of 54 mm ×

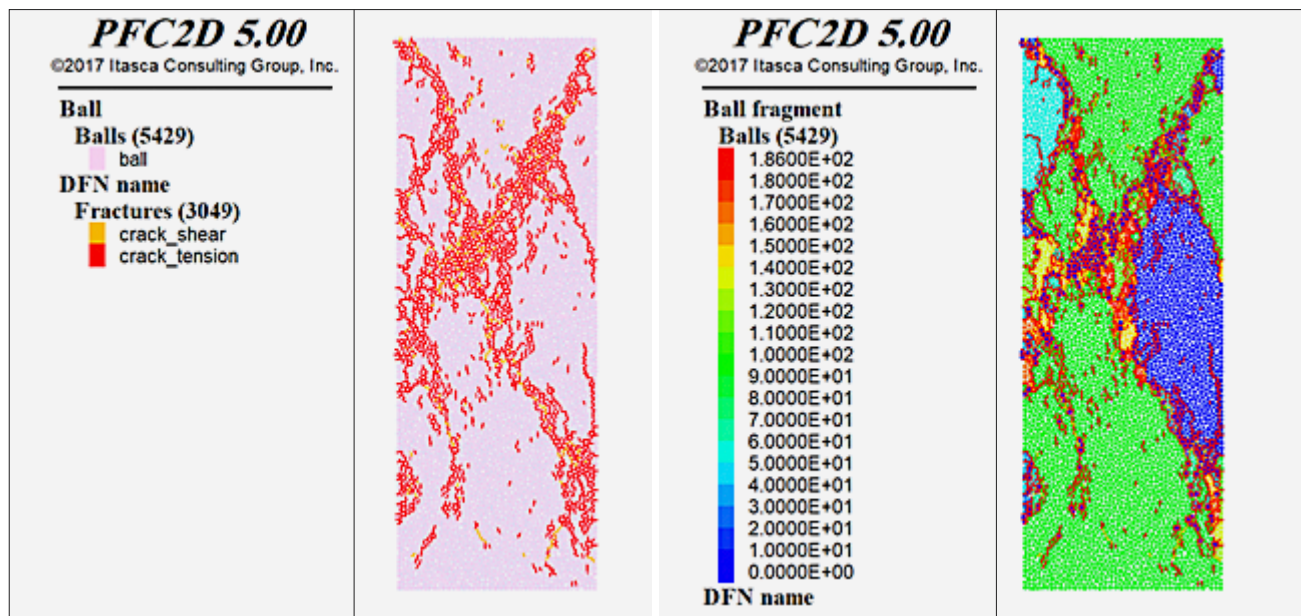


150 mm were cast and cured under standard laboratory conditions for 28 days. The specimens were tested using a universal testing machine with a loading rate of 0.5–1.0 MPa/s until failure occurred. The compressive strength was calculated by dividing the maximum applied load by the cross-sectional area of the specimen. Three specimens were tested for this property, and the

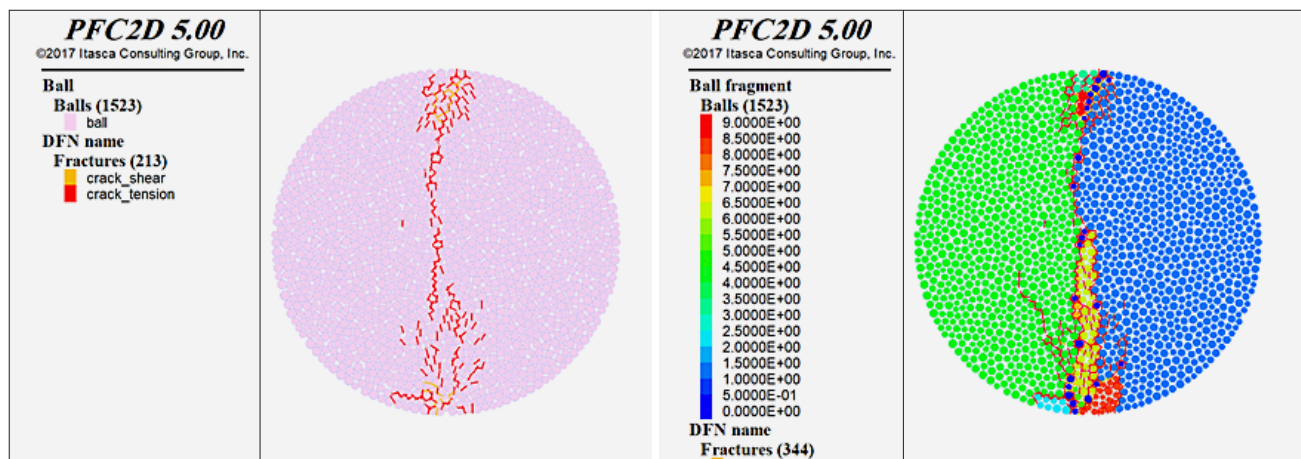
**Table 2:** Rock mechanical properties of the concrete sample used

Parameter	Unit	Value
Density	Kg/m <sup>3</sup>	2240
Uniaxial compressive strength	MPa	30
Tensile strength	MPa	3.5
Modulus of elasticity	GPa	20
Poisson's ratio	-	0.2
Shear strength	MPa	10

values presented in **Table 2** represent their average. Indirect tensile strength of the concrete was determined using the Brazilian test, as per the ISRM-suggested method for “Determination of Tensile Strength by the Brazilian Test” on 28-day concrete disk samples being 54 mm in diameter and 27 mm in length. In this method, cylindrical specimens were subjected to diametral compression in a universal testing machine. The applied load created tensile stress perpendicular to the loading direction until failure occurred. The tensile strength was calculated using the formula  $\sigma_t = \frac{2F}{\pi LD}$ , where F is the maximum load applied, L is the length of the specimen, and D is the diameter. **Ten specimens** were tested for this property to ensure greater accuracy, and the values in **Table 2** represent their average. For the density, it was determined by measuring the weight and volume of the specimens and calculating the ratio of mass to volume. The ISRM-suggested method for “Determination of



**Figure 1:** Calibration of Uniaxial Compressive Strength of tested concrete in PFC Software



**Figure 2:** Calibration of Indirect tensile strength of tested concrete in PFC Software

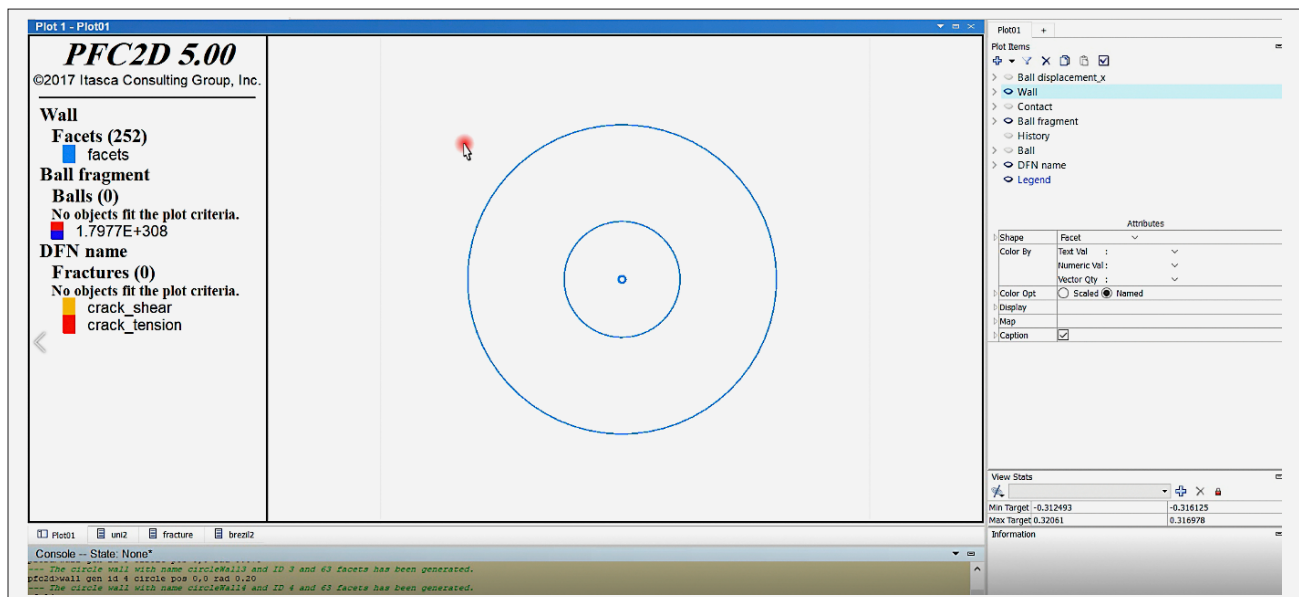


Figure 3: Construction of main wall of the model

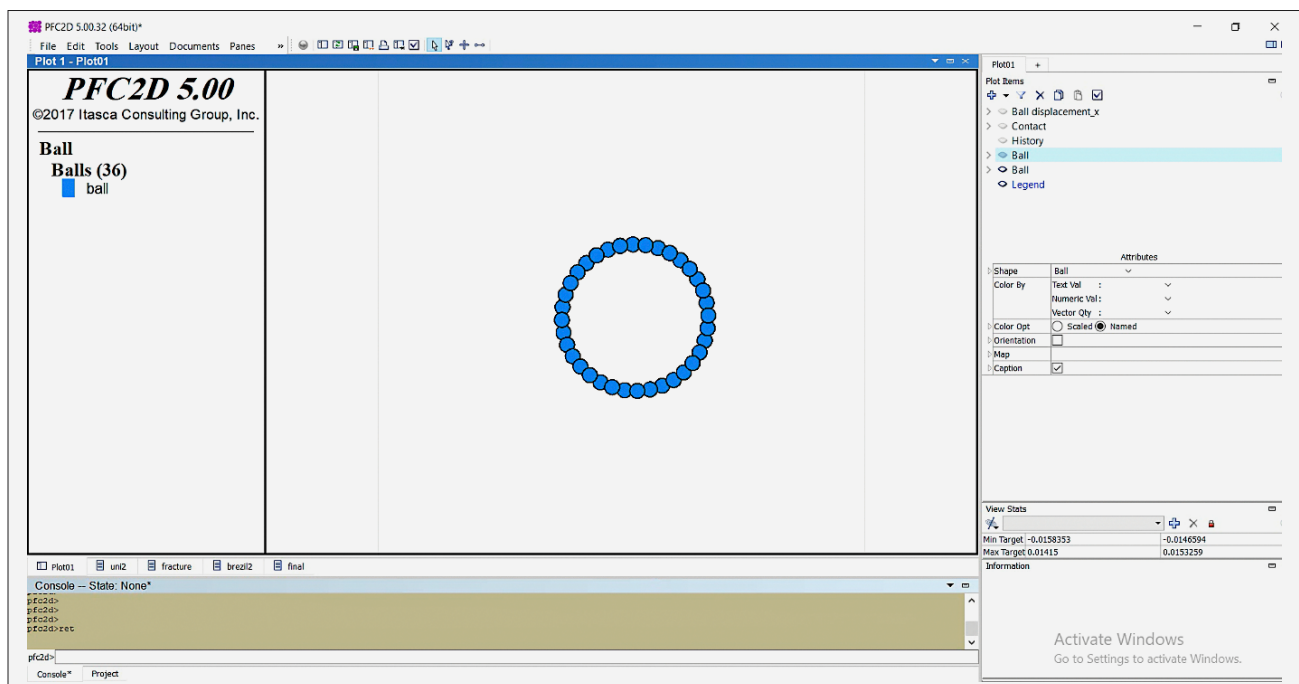


Figure 4: Construction of copper pipe geometry

Density of Rock Materials” was followed. Three specimens were tested, and the average value is reported in **Table 2**. The modulus of elasticity and Poisson’s ratio were obtained from stress-strain measurements during uniaxial compressive testing, in accordance with the ISRM-suggested method for “Determination of Elastic Moduli”. Strain gauges were used to measure longitudinal and lateral strains, enabling the calculation of Poisson’s ratio as the ratio of lateral strain to longitudinal strain in the elastic region. Three specimens were used for these measurements, and the average values are presented in **Table 2**. The shear strength of the concrete was

evaluated using the ISRM-suggested method for «Shear Testing of Rock Samples.» Cylindrical specimens were subjected to shear forces until failure occurred, and the maximum load was divided by the area of failure to calculate shear strength. Three specimens were tested, and the average value is reported in **Table 2**. After obtaining the experimental results, the mechanical properties, including uniaxial compressive strength, tensile strength, density, modulus of elasticity, Poisson’s ratio, and shear strength, were used as input parameters for simulation in the Particle Flow Code (PFC) software. The calibration process involved adjusting the PFC model parameters to



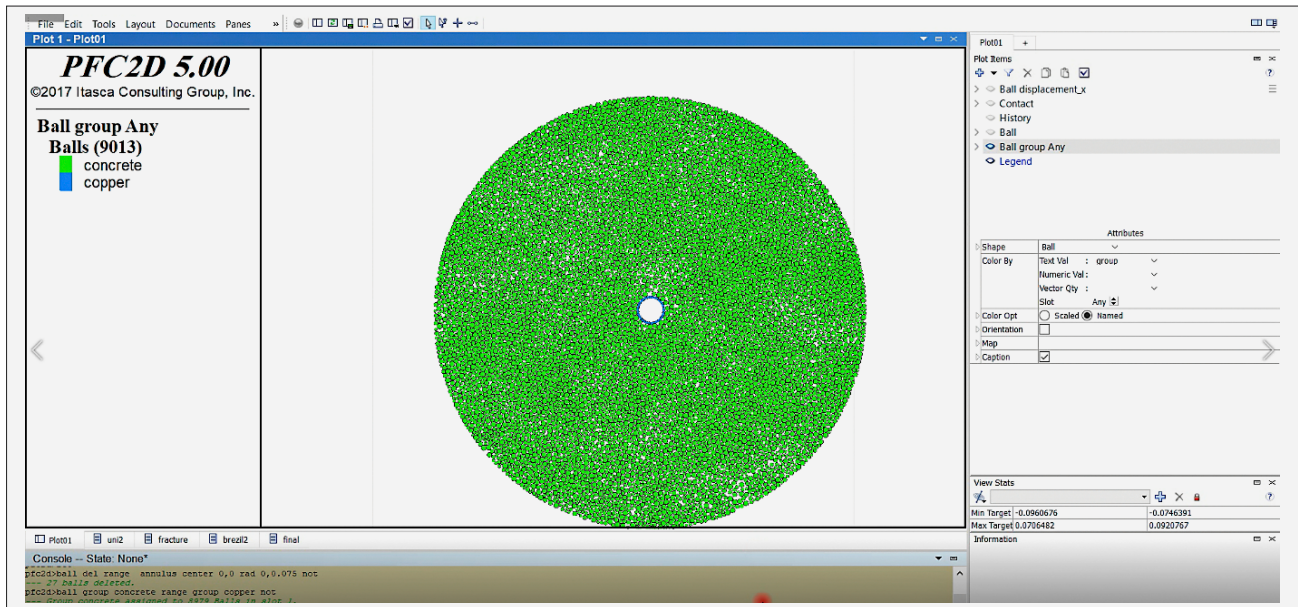


Figure 5: Showing the construction of concrete sample model with copper pipe

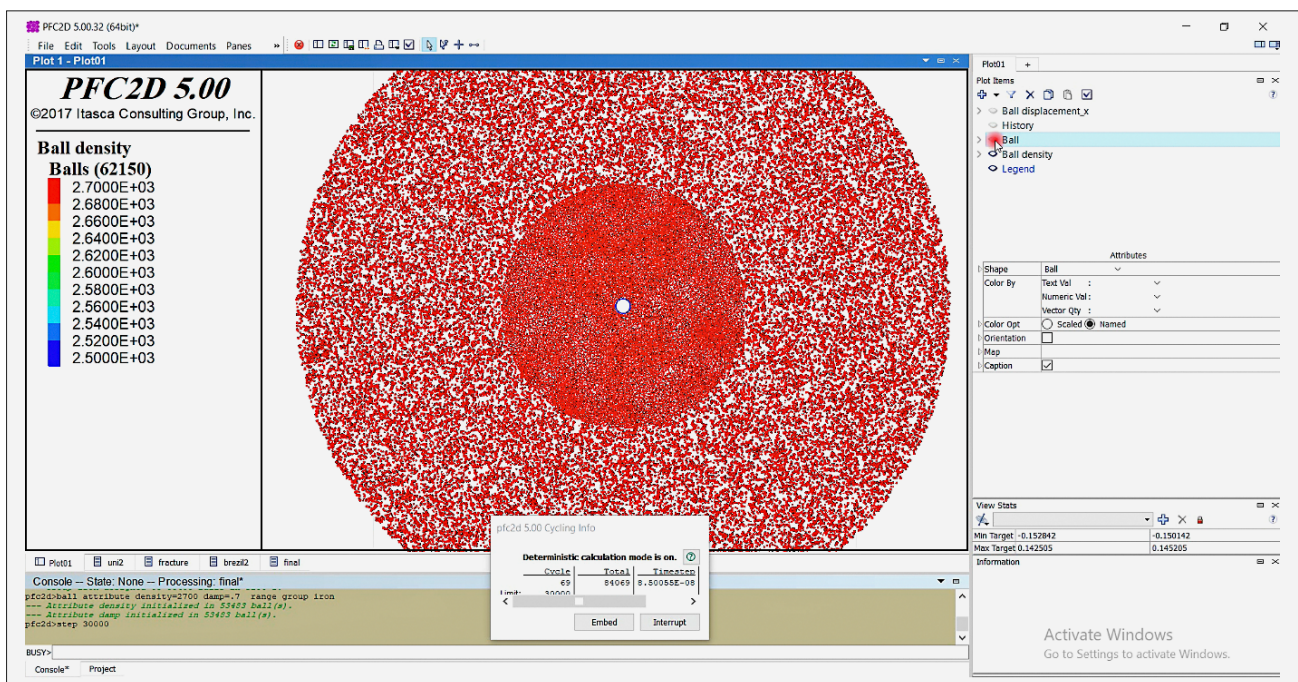


Figure 6: The construction of the concrete sample model, the copper pipe, and the iron powder

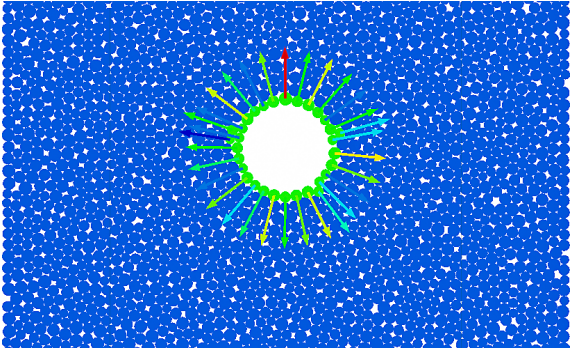
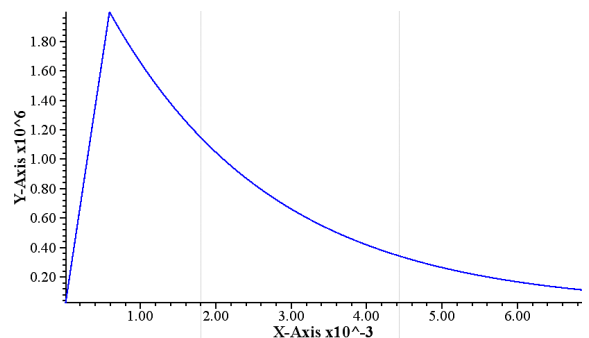
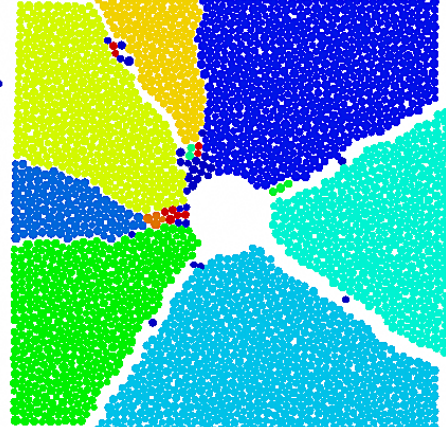

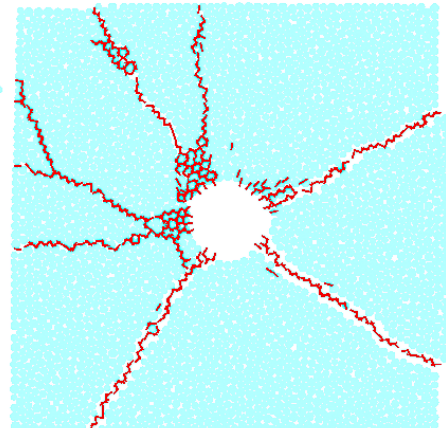
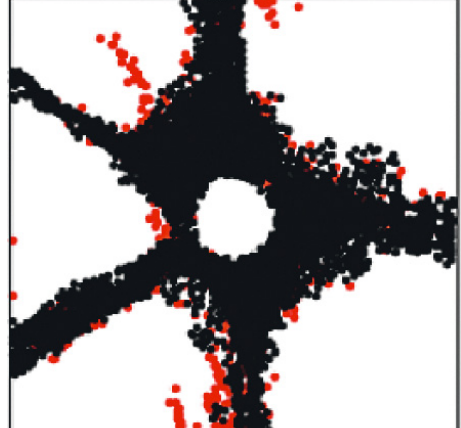
match the experimental results, ensuring accurate representation of the concrete's mechanical behaviour. **Figure 1** and **Figure 2** illustrates an example of modelling and calibration of uniaxial compressive strength and tensile strength within the PFC software.

## 2.2. Development of numerical modelling

As previously mentioned, the energy resulting from the explosion comprises shock (the shock applied to the hole), reflection (the energy that returns), and gas pressure (the pressure caused by the explosion in the cracks

formed in the rock). The objective of this section is to investigate the impact of each of these waves on the extent of rock fragmentation. Shock energy is present in all parts and models created, but reflection and gas pressure can be mitigated through specific methods. A blasting chamber is constructed, and a concrete sample is positioned inside for the blasting operation. In essence, a cylindrical explosion chamber is used, containing a concrete sample with a 1 cm hole and a copper tube with an 8 mm diameter to alleviate the gas pressure. In the initial stage, these parameters are incorporated into the numerical model (see **Figure 3** and **Figure 4**).

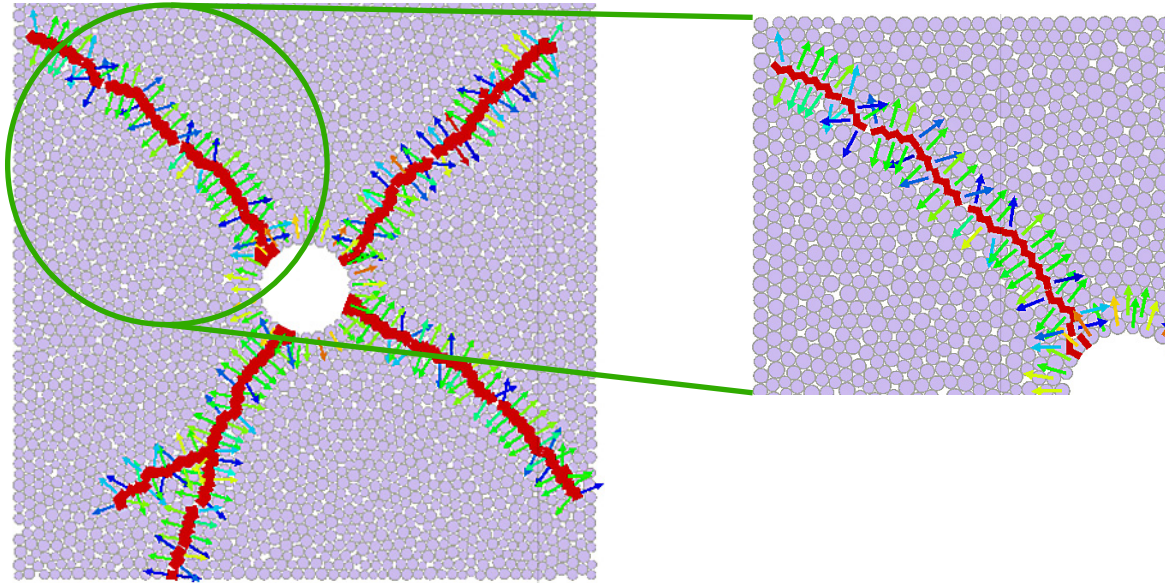
**Table 3:** Validation of the developed model based on the study conducted in this field in the PFC software environment

Results of this study	Results of the software manual
 <p>Application of radial forces dependent on grain size</p>	 <p>Plot of gas pressure (Pa) in terms of time (S)</p>
 <p>Fragments from the explosion</p>	 <p>Fragments from the explosion</p>
 <p>Crack growth process</p>	 <p>Crack growth process</p>

In the subsequent stage, the concrete geometry is established. During this phase, the barrier separating the concrete and the copper pipe is eliminated, ensuring their complete connection. In this scenario, the copper pipe functions as a solid wall (see **Figure 5**). Subsequently, the properties of the concrete grains are integrated into the model, and following that, the primary type of concrete (properties obtained from the calibration stage) is introduced into the model.

When a copper pipe is present, it effectively prevents the transmission of gas pressure after the explosion, resulting in a reduction of gas pressure to zero. The rationale behind selecting a copper pipe is its ability to maintain an elastic state and undergo shape changes without tearing, thereby preventing gas from escaping. Subsequently, the modelling of iron powder is carried out. In a manner similar to the previous step, the boundary between the iron and concrete is removed. It's important to





**Figure 7:** The directions of crack propagation and the application of vertical gas pressure to it

note that the iron used in this experiment is granular, and the model's behaviour is linear, thus necessitating different instructions for creating the iron model compared to copper and concrete. Following the explosion, cracks and wave propagation occur, with these waves impacting the model's boundary. If the reflected energy strikes a solid wall, it creates a crack. However, if it encounters the iron powder, which can move freely, it explodes and transforms into heat due to friction between the iron powder and the wave. Consequently, the reflected energy is reduced to zero. **Figure 6** shows the construction of the concrete sample model, the copper pipe, and the iron powder.

### 2.3. Validation of the model

To validate the Particle Flow Code (PFC) software, the results of PFC software have been used. This study involves simulating the explosion of a hole in a homogeneous, isotropic, elastic rock environment. **Table 3** presents the outcomes obtained from modelling the concrete sample under investigation and the results derived from manual modelling. As indicated in the table, a strong concordance is observed between this study and the software test results.

### 2.4. Development of the function code for applying gas pressure in the produced cracks

In this section, the gas pressure function has been developed and the gas has been modelled for the first time. This sector faces two major challenges, which include the propagation of cracks and the application of gas pressure perpendicular to these cracks. In general, there is no rock mechanics software that models gas (or any other type of fluid) inside the rock. In other words, there is a void where cracks were created and spread inside

after the explosion, and inside these cracks, gas must be modelled. The primary issue is that the fluid always exerts pressure vertically. Therefore, in the written code, the crack direction is first determined, and then gas pressure is applied perpendicular to it. Finally, a code for initiating the explosion is incorporated into the model. This code facilitates the process of applying gas pressure to the cracks produced during the explosion. The operation of this code can be described as follows:

- The gas pressure within the cracks formed during the explosion is a function of time, and it's applied in accordance with the pressure-time diagram defined by the user for the explosion.
- Bands or connections that break under loading receive the pressure from the explosive gas. This pressure is applied as a force vector to the spheres around the crack, acting perpendicular to the crack (hydrostatically), and it tends to open the crack.
- The conversion of gas pressure within a crack into the force applied to the spheres is determined by a quarter of the sphere's circumference, which represents the active surface in contact with the crack or gas pressure. Consequently, even if there is a constant gas pressure within the crack, the difference in radius between two spheres around a crack results in varying forces being applied to these spheres.
- Since multiple cracks may surround a single sphere, the code adjusts the magnitude and direction of the applied force while calculating the gas forces applied to this sphere. This becomes particularly crucial in models with numerous cracks, and it can slow down the model. To address this issue, a robust analysis system is required. It might be possible to enhance speed by dedicating more time to the analysis process.



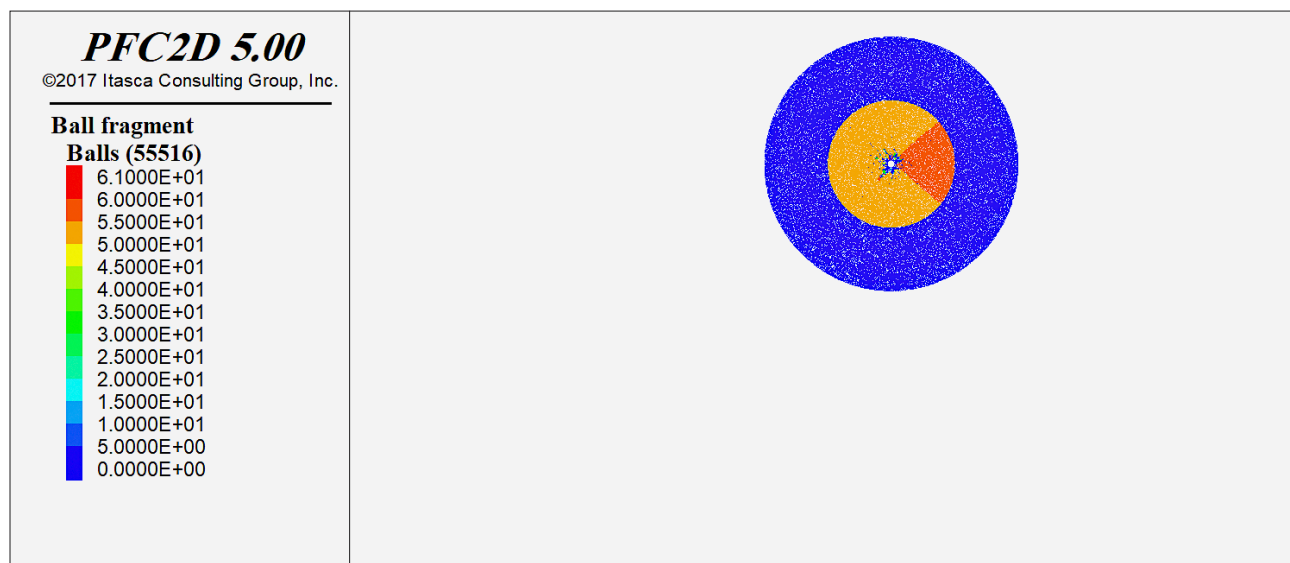


Figure 8: Generated fragments during the simulation of shock energy modelling

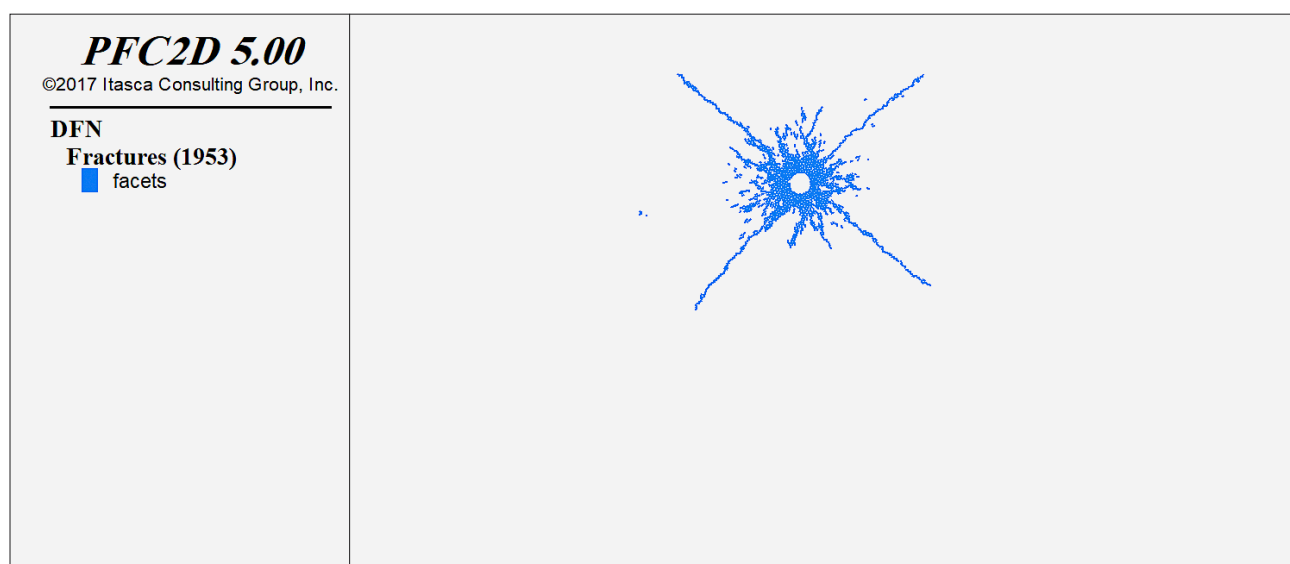


Figure 9: Propagation of cracks induced by shock energy during the simulation

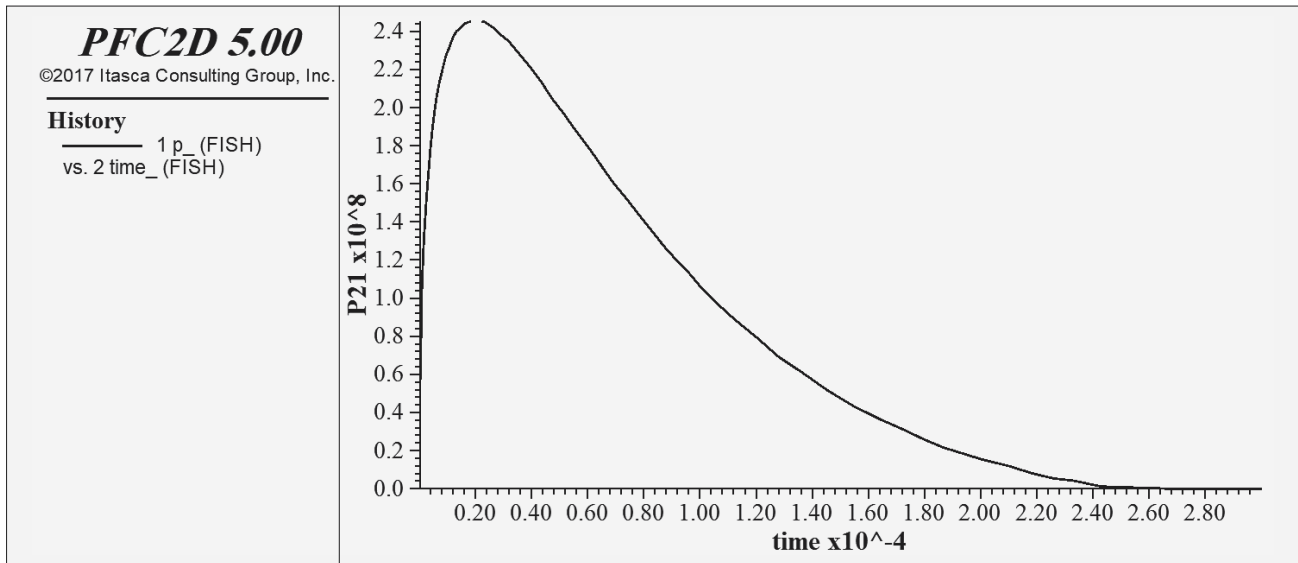
Finally, the output observed after implementing this code is the simulation of the crack branching phenomenon, which is considered a significant advancement in PFC. **Figure 7** shows the directions of crack propagation and the application of vertical gas pressure to it.

The methodology adopted in this study involves the development of a unique code within the PFC environment to simulate gas pressure effects in fractures. Unlike traditional models, which often assume uniform or isotropic gas pressure distribution, our approach dynamically calculates the orientation of each crack and applies pressure perpendicularly to its surface. This process ensures that the interaction between the explosive gases and the rock material is represented with high fidelity. Moreover, the code accounts for variations in gas pressure over time, simulating the decay of pressure as the gases escape through fractures. This time-dependent be-

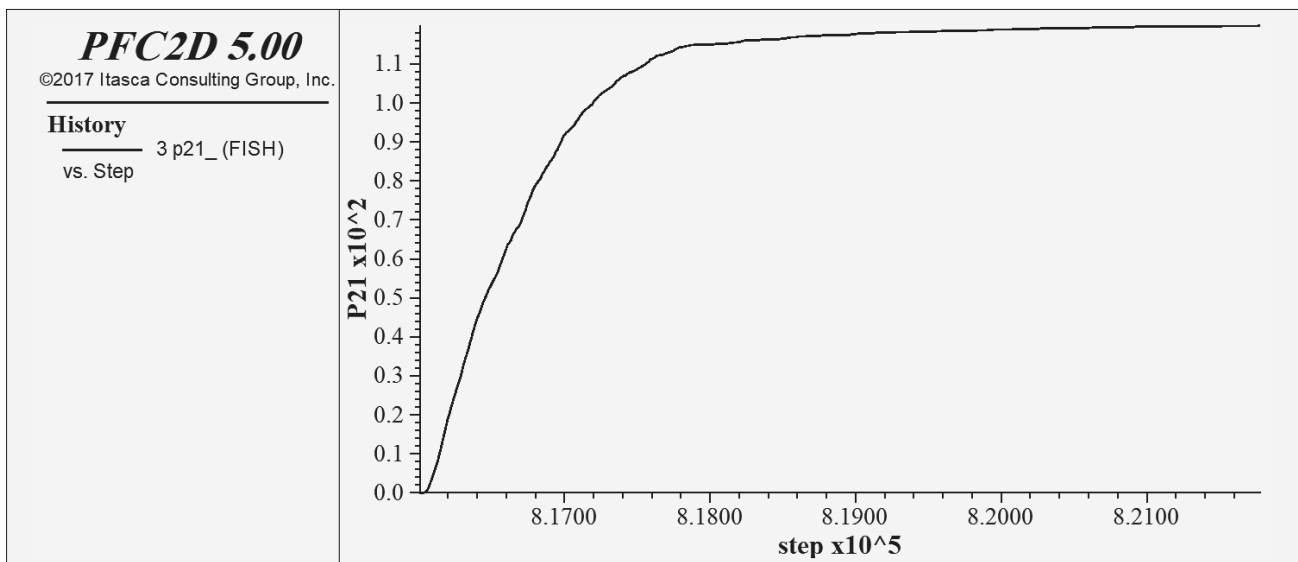
haviour adds a new dimension of realism to the simulation, allowing for a better understanding of how gas pressure contributes to crack propagation and fragmentation efficiency. The challenges encountered during this development, including computational limitations and the need for precise calibration, were overcome through iterative testing and refinement. This innovative approach not only enhances the predictive capabilities of PFC but also establishes a framework for integrating fluid dynamics into discrete element modelling.

### 3. Numerical modelling results

To assess the extent of fragmentation resulting from the explosion under various conditions such as shock, reflection, gas pressure, and the absence of blast energy, joint density is employed. This assessment is based on



**Figure 10:** Blast diagram illustrating energy dissipation and shockwave dynamics in the presence of shock energy



**Figure 11:** Joint density diagram highlighting the fragmentation process during shock energy modelling

the data obtained from P21 plot, which represents the total length of discontinuities per unit surface area ( $\text{m}/\text{m}^2$ ). The construction of this plot has been achieved through coding in the PFC3D software environment. This model has been established for all areas as follows.

### 3.1. Modelling in the presence of copper pipe and iron powder

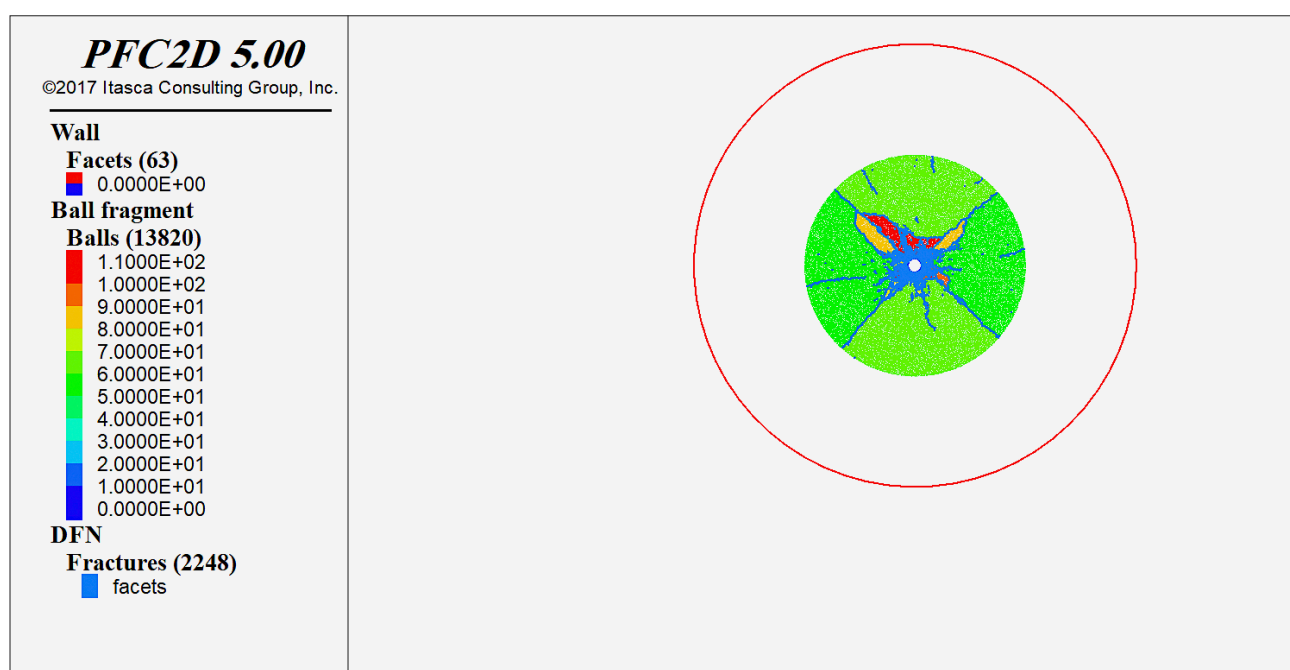
In this scenario, only the shock energy is being modelled. The simulation results for this scenario are presented in **Figures 8 to 11**. **Figure 8** illustrates the distribution and size of the generated fragments, demonstrating the fragmentation process. **Figure 9** highlights the propagation of cracks, showing the pathways and spread induced by the shock energy. **Figure 10** depicts the blast diagram, visualizing the dissipation of energy and shock-

wave dynamics. Finally, **Figure 11** displays the joint density, emphasizing the fragmentation process.

As observed in **Figures 8 to 11**, a high density of fractures has formed around the blast hole, with four distinct groups of longer fractures evident in the vicinity of the hole. It is clear that complete disintegration has not occurred in the model; instead, the shock wave energy has primarily caused the formation of initial fractures. This observation aligns well with existing theories and previous studies, which suggest that the initial energy from blasting typically induces micro-fracturing and crack propagation rather than immediate and complete disintegration of the rock mass. In this scenario, as depicted in the figures, the total number of fractures generated is 1953, and the cumulative length of discontinuities formed is 110 meters per square meter. These findings indicate that the energy from the blast was effectively



**Figure 12:** Distribution and size of the generated fragments during the simulation of shock and reflection energy



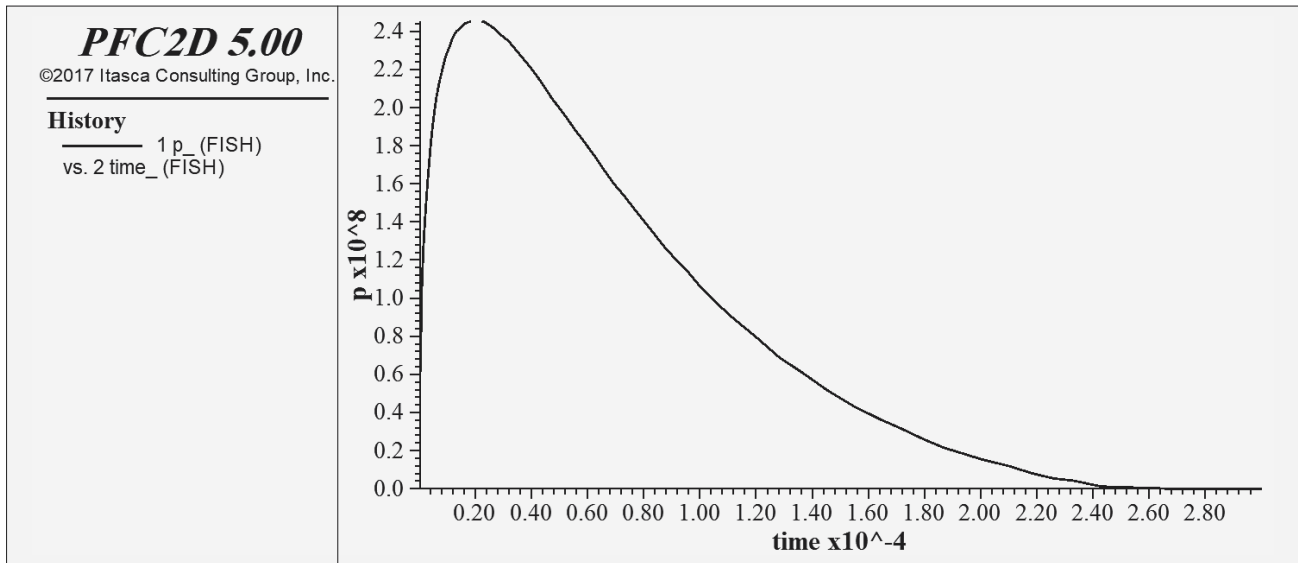
**Figure 13:** Propagation of cracks induced by shock and reflection energy during the simulation of the second state

transferred into the surrounding material, creating a fracture network that could significantly influence subsequent rock fragmentation and stability. These results provide valuable insight into the early stages of fracture development around blast holes and emphasize the role of shock wave energy in initiating micro-fractures. Such detailed modelling helps in understanding the mechanics of rock breakage and can inform the optimization of blasting parameters to achieve desired fragmentation with minimal environmental and operational impact.

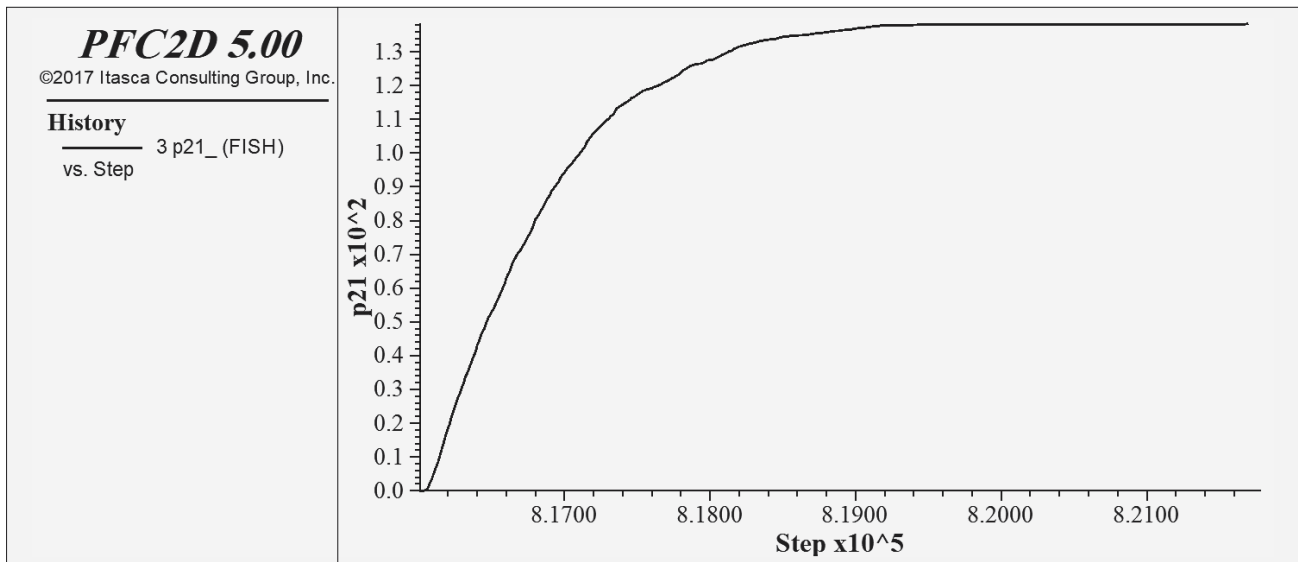
### 3.2. Modelling in the presence of copper pipe

In this scenario, only shock and reflection energy is modelled. The simulation results for this state are presented in **Figures 12 to 15**. **Figure 12** illustrates the distribution and size of the generated fragments, showing the fragmentation process. **Figure 13** highlights the propagation of cracks, demonstrating the pathways and spread induced by shock and reflection energy. **Figure 14** depicts the blast diagram, visualizing the dissipation





**Figure 14:** Blast diagram illustrating energy dissipation and shockwave dynamics in the presence of shock and reflection energy

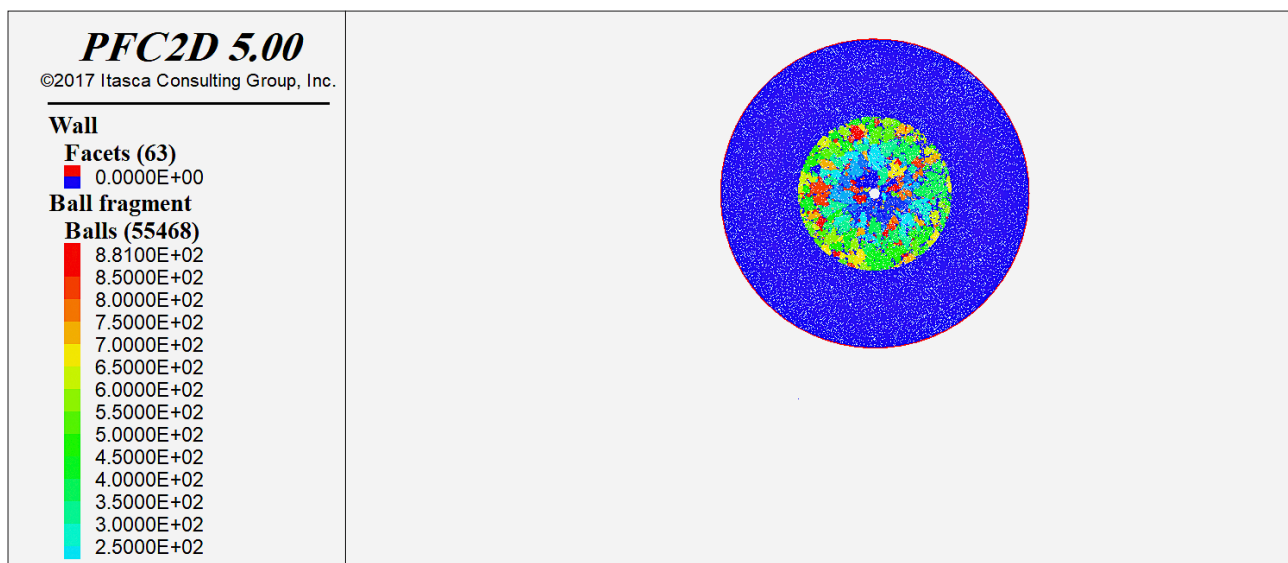


**Figure 15:** Joint density diagram showing the variation of joint density over time and its relation to the fragmentation process during the simulation of shock and reflection energy

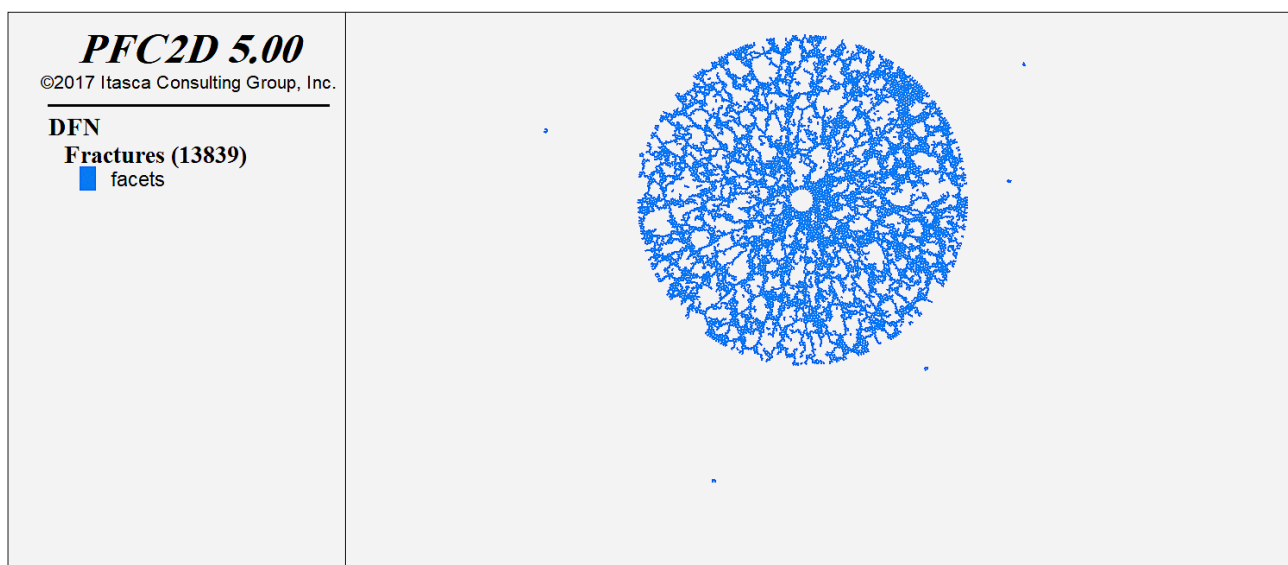
of energy and shockwave dynamics. Finally, **Figure 15** presents the joint density diagram, showing the variation of joint density over time and its relationship with the fragmentation process during the simulation of the second state with shock and reflection energy.

As observed in **Figures 12 to 15**, similar to the simulation involving shock energy alone, a high density of fractures has formed around the blast hole, with four distinct groups of longer fractures visible near the hole. Additionally, micro-fractures are observed in the outer region of the model, which can be attributed to the effect of reflected energy. According to the obtained graphs, the total number of fractures in this scenario is 2,248, and the cumulative length of discontinuities is 130 meters per square meter. This represents an increase of less

than 20% compared to the case of shock energy alone. The results indicate that while the presence of reflected energy contributes to additional fracture formation, its impact remains secondary to that of the primary shock energy. Considering that the model remained intact in both simulations, it can be concluded that the primary role of both shock energy and reflected waves is the initiation and propagation of fractures in the rock rather than complete disintegration. This finding underscores the importance of understanding energy transfer mechanisms during blasting operations, as it highlights the distinct contributions of different wave types to fracture dynamics. Such insight is crucial for optimizing blasting parameters to control fragmentation and minimize adverse effects on the surrounding environment.



**Figure 16:** Distribution and size of the generated fragments during the simulation of shock energy and gas pressure

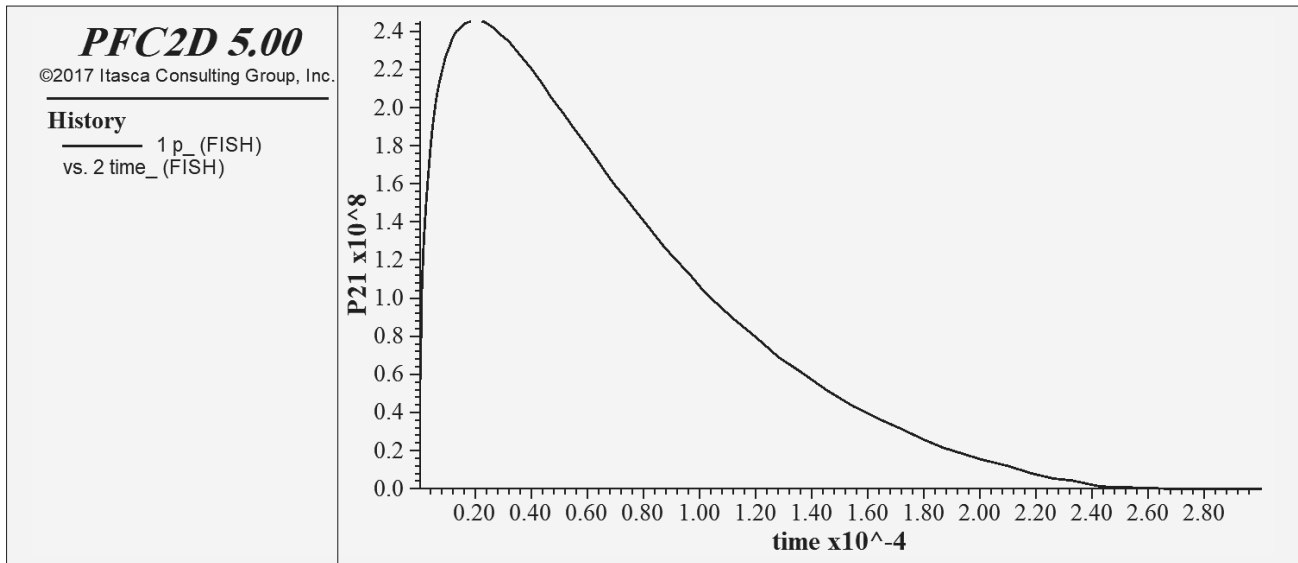


**Figure 17:** Propagation of cracks induced by shock energy and gas pressure during the simulation of the third state

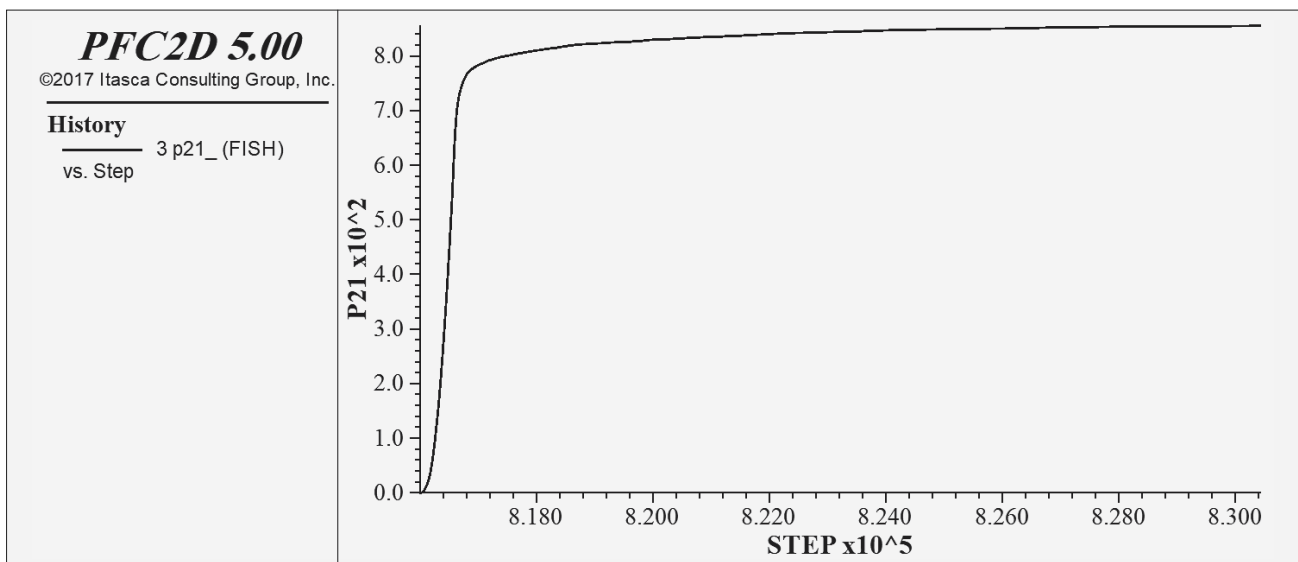
### 3.3. Modelling in the presence of iron powder

In this scenario, only shock energy and gas pressure are modelled. The simulation results for this state are presented in **Figures 16 to 19**. **Figure 16** illustrates the distribution and size of the generated fragments, showing the fragmentation process. **Figure 17** highlights the propagation of cracks, demonstrating the pathways and spread induced by shock energy and gas pressure. **Figure 18** depicts the blast diagram, visualizing the dissipation of energy and shockwave dynamics. Finally, **Figure 19** presents the joint density diagram, showing the variation of joint density over time and its relation to the fragmentation process during the simulation of the third state with shock energy and gas pressure.

As observed in **Figures 16 to 19**, unlike the two previous models, the continuity of the material has been lost in this scenario, resulting in a highly fragmented zone. In this model, the density of fractures has significantly increased, and the blasting process has progressed to completion, as expected under these conditions. According to the obtained graphs, the total number of fractures generated is 13,839, and the cumulative length of discontinuities has reached approximately 850 meters per square meter. Compared to the previous two models, these figures represent a roughly sevenfold increase in both the number of fractures and the cumulative length of discontinuities. This dramatic rise highlights the critical role of gas pressure in the blasting process, as it greatly amplifies fracture density and ensures complete fragmentation



**Figure 18:** Blast diagram illustrating energy dissipation and shockwave dynamics in the presence of shock energy and gas pressure



**Figure 19:** Joint density diagram showing the variation of joint density over time and its relation to the fragmentation process during the simulation of shock energy and gas pressure

of the material. These results emphasize the importance of considering gas pressure in the simulation and optimization of blasting operations. The substantial increase in fracture metrics demonstrates that gas pressure not only extends the reach of fractures but also transforms the rock into a fully fragmented zone, which is essential for efficient material extraction. Future studies could further explore the interplay between gas pressure, shock energy, and material properties to optimize the balance between energy efficiency and fragmentation outcomes in blasting processes.

### 3.4. Modelling without the presence of copper pipe and iron powder

In this scenario, all three energies of shock, reflection and gas pressure are modelled. The simulation results

for this state are presented in **Figures 20 to 23**. **Figure 20** illustrates the distribution and size of the generated fragments, showing the fragmentation process. **Figure 21** highlights the propagation of cracks, demonstrating the pathways and spread induced by shock, reflection, and gas pressure. **Figure 22** depicts the blast diagram, visualizing the dissipation of energy and shockwave dynamics. Finally, **Figure 23** presents the joint density diagram, showing the variation of joint density over time and its relation to the fragmentation process during the simulation of the fourth state with all three energies.

As observed in **Figures 20 to 23**, the model in this simulation has undergone complete fragmentation. In this scenario, the total number of fractures generated is 17,673, and the cumulative length of discontinuities has reached 1,100 meters per square meter. Compared to the



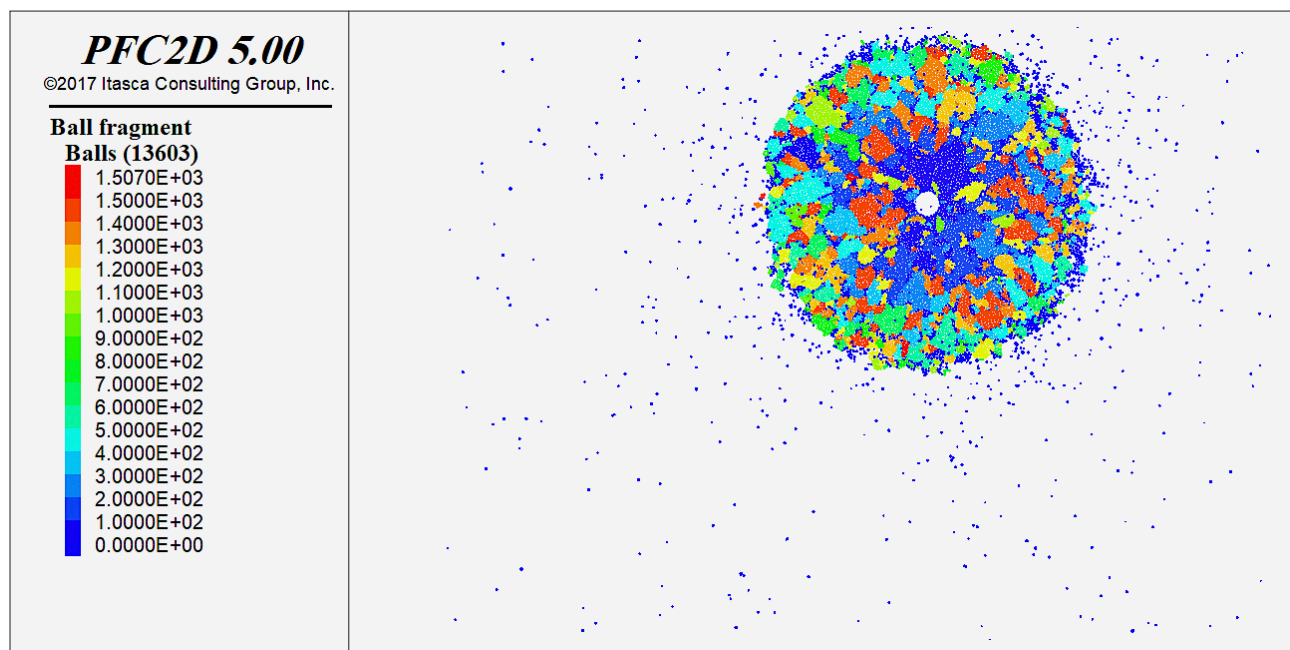


Figure 20: Distribution and size of the generated fragments during the simulation of shock, reflection, and gas pressure

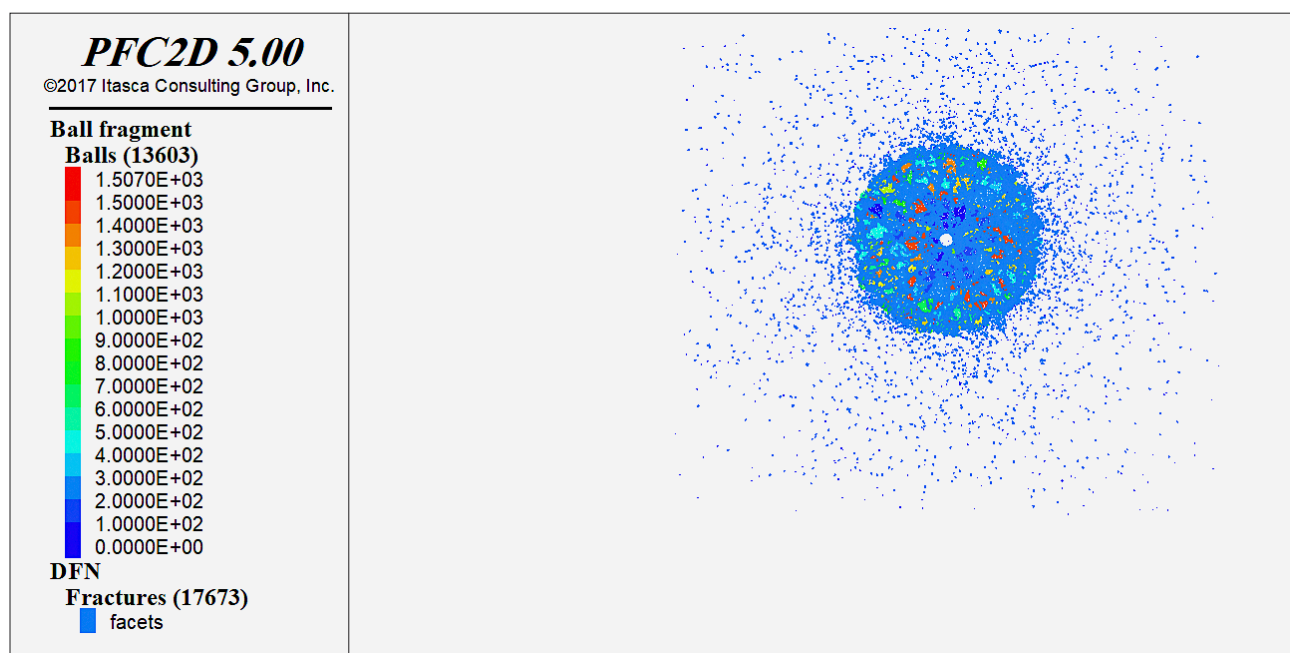
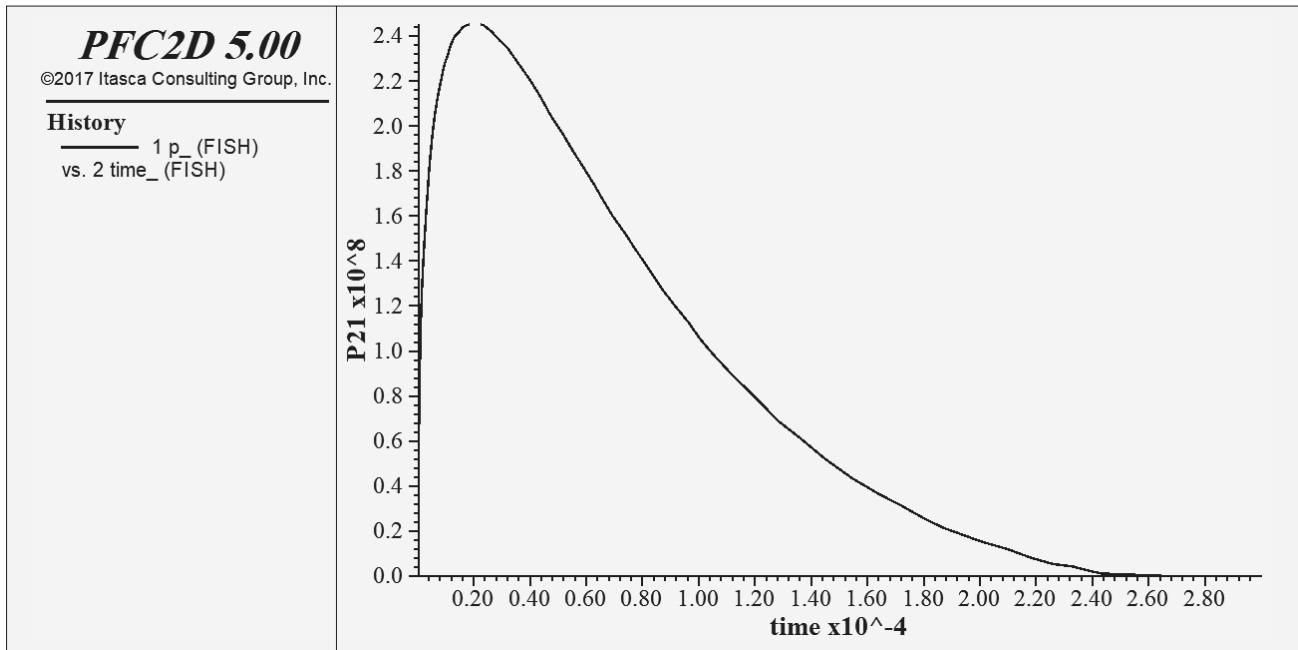


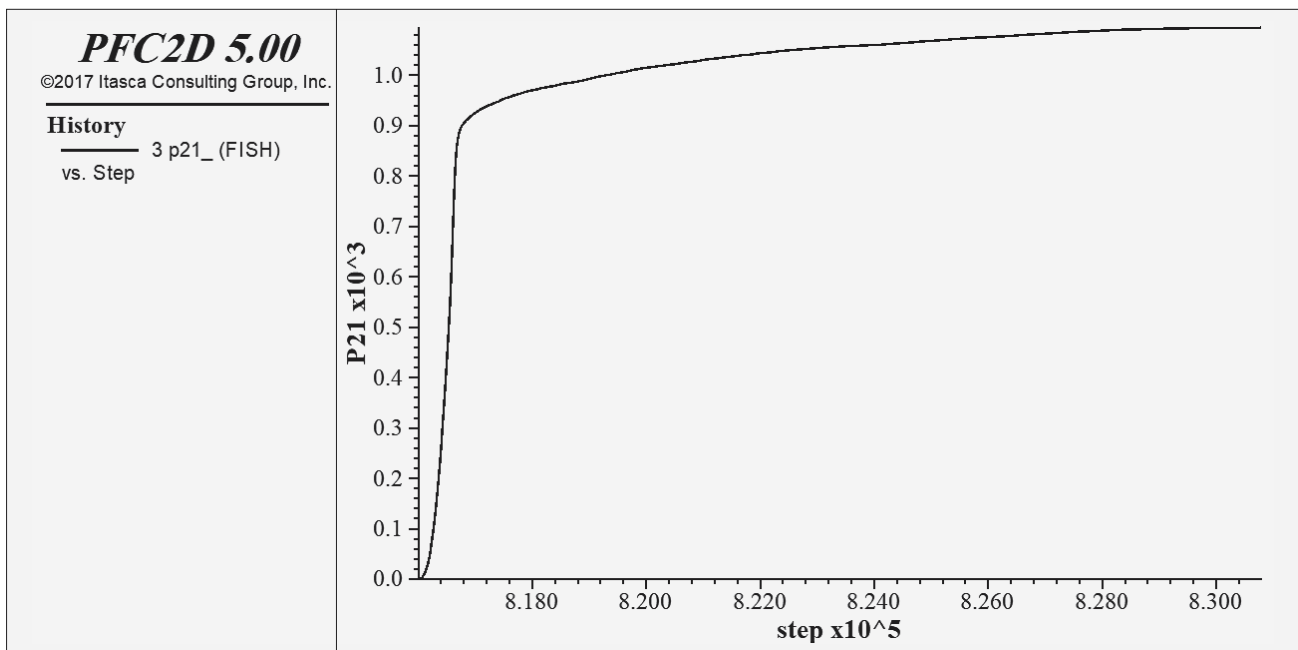
Figure 21: Propagation of cracks induced by shock, reflection, and gas pressure during the simulation of the fourth state

cases without gas pressure, this model shows approximately a ninefold increase in the number of fractures and a tenfold increase in the cumulative length of discontinuities. Furthermore, when compared to the case with gas pressure but without reflected energy, an increase of about 30% is observed in both the number of fractures and the cumulative length of discontinuities. This highlights the significant role of reflected waves in enhancing the fragmentation process during blasting. These results underscore the combined influence of gas pressure and reflected energy in achieving efficient and complete

rock fragmentation. The reflected waves not only amplify fracture density but also enhance the propagation of discontinuities, contributing to a more effective blasting outcome. Understanding the synergistic effects of these energy components is crucial for optimizing blasting designs and improving fragmentation efficiency while minimizing energy waste. Future research should explore these interactions further in real-world conditions to validate and refine these findings.



**Figure 22:** Blast diagram illustrating energy dissipation and shockwave dynamics in the presence of shock, reflection, and gas pressure



**Figure 23:** Joint density diagram showing the variation of joint density over time and its relation to the fragmentation process during the simulation of shock, reflection, and gas pressure

## 4. Discussion

The modelling results under different explosion scenarios reveal that radial cracks are initiated by the initial shock wave and further develop within the rock. As the reflected wave passes through, these cracks can absorb more energy and expand further. In the final stage, the release of gas leads to the fracturing of the rock. Furthermore, the modelling results indicate that the shock wave

has a substantial impact on the formation of the majority of cracks within the sample. While the increased presence of gas does contribute to exerting pressure on the resulting rock fragments, its effect is less significant compared to the initial shock wave. Both the shock wave and gas pressure play essential roles in the rock fragmentation process during an explosion. It is worth noting that the reflected pressure has the least influence on crack expansion within the rock, making the smallest

contribution to the process. These findings align well with the research conducted by other scholars (**Banadaki and Mohanty, 2014; Lanari and Fakhimi, 2015**).

This study introduces a paradigm shift in the modelling of blast-induced rock fragmentation by emphasizing the critical role of gas pressure. The function developed within the PFC framework has successfully demonstrated its ability to simulate the complex interactions between shock energy, reflected waves, and gas pressure. While the current study focuses on the simulation and mechanical characterization of concrete samples as an analogue for rock, future work will aim to extend the methodology to real rock samples. Real rock materials present unique challenges, such as heterogeneity, anisotropy, and variability in mechanical properties, which can significantly affect the outcomes of blasting and crushing operations. Setting up small-scale experiments on real rock samples would enable validation of the numerical model's applicability under more realistic conditions and allow for fine-tuning of the input parameters to better replicate field scenarios. It is important to emphasize that numerical modelling serves as an essential preliminary step in understanding complex processes such as rock blasting and crushing. These simulations allow researchers to predict the overall behaviour of materials under controlled conditions, offering valuable initial insight without the need for costly and time-consuming full-scale experiments. The modelling approach used in this study provides a detailed representation of the mechanical behaviour of the material, enabling the investigation of various scenarios, parameter adjustments, and energy variations in a highly controlled and repeatable environment. By combining laboratory-based calibration and numerical modelling, we have developed a framework that bridges experimental findings with predictive simulations. This not only helps in optimizing the experimental design but also reduces the overall cost and resource consumption associated with real-world testing. Numerical simulations are particularly advantageous for identifying potential challenges and refining processes before conducting more extensive experiments on real rock samples. In future studies, the integration of real rock sample testing with advanced numerical modelling will further enhance the robustness and applicability of this research. Such an approach ensures a comprehensive understanding of the process while leveraging the strengths of both experimental and computational methods.

## 5. Conclusions

This study focuses on comprehending the mechanisms behind rock blasting using explosives and evaluating their influence on crack growth and rock crushing. Employing numerical analysis through PFC software, the research investigates explosion mechanisms and their effects on crack development. It begins by incorpo-

rating laboratory-tested concrete sample data into the model and calibrating numerical parameters based on prior research. The study explores four explosion modes in a concrete sample with a blast hole, considering shock energy, reflection, and gas pressure individually and in combinations. Key findings of the study include:

1. The results show that the simultaneous inclusion of shock energy, reflection, and gas pressure leads to the highest density of fractures, resulting in the greatest rock fragmentation. This demonstrates that combining these energies can significantly enhance the efficiency of the blasting process and optimize the explosion mechanisms. The analysis also accurately examined how energy is distributed within the rock and the propagation of cracks in different directions.
2. Comparing the different models revealed that the model with both gas pressure and shock energy produced the highest level of rock fragmentation. In contrast, models incorporating only shock and reflection energies or shock energy alone resulted in less fragmentation. These results were further confirmed through analysis of fragmented rock images and crack propagation.
3. One of the key findings of this study is the substantial effect of gas pressure on rock fragmentation. Gas pressure increased rock fragmentation by up to 7.7 times compared to when only shock energy was present. Furthermore, the presence of all three energies (shock, reflection, and gas) led to an increase in fragmentation by 1.3 to 10 times compared to the models with only shock and gas pressure or shock energy alone. These results highlight the crucial role of gas pressure in enhancing rock crushing behaviour during explosions.
4. The study also examined how cracks initiate and propagate within the rock. It was found that shock energy is responsible for creating initial radial cracks, while gas pressure plays a critical role in extending and deepening these cracks. The models that combined shock, reflection, and gas energies exhibited more complex and effective crack propagation mechanisms. The number of cracks formed in different models varied significantly, with the combination of all three energies resulting in the highest number of cracks.

The findings of this study can have significant practical applications in optimizing blasting operations in mining and industrial projects. By utilizing these results, it is possible to reduce the consumption of explosives and prevent unpredictable and unstable explosions. Furthermore, future research should focus on field testing and validating these simulations under real-world conditions. Further studies exploring the combined effects of blasting energies in various geological settings and employing more sophisticated models could further improve the accuracy and efficiency of these processes.



## 6. References

- Jimeno, C. L., Jimeno, E. L. and Carcedo, F. J. A. (1995): Drilling and blasting of rocks. AA Balkema: Rotterdam, The Netherlands, 391 p.
- Banadaki, M. and Mohanty, B. (2014): Numerical simulation of stress wave induced fractures in rock. *International Journal of Impact Engineering*, 16–25. <https://doi.org/10.1016/j.ijimpeng.2011.08.010>.
- Bhandari, S. (1997): Engineering rock blasting operations. AA Balkema: Rotterdam, The Netherlands, 375 p.
- Chi, L. Y., Zhang, Z. X., Aalberg, A., Yang, J. and Li, C. C. (2019): Measurement of shock pressure and shock-wave attenuation near a blast hole in rock. *International Journal of Impact Engineering*, 125, 27–38. <https://doi.org/10.1016/j.ijimpeng.2018.11.002>.
- Fourney, W. (1993): Mechanisms of rock fragmentation by blasting. In: Hudson J. A. (ed.): *Comprehensive rock engineering, principles, practice and projects*. Seoul Pergamon Press, 1st ed., vol. 4., Oxford: New York, 39–69, 982 p.
- Kutter, H. K. and Fairhurst, C. (1971): On the fracture process in blasting. *International Journal of Rock Mechanics and Mining Sciences & Geomechanics Abstracts*, 8(3), 181–202. [https://doi.org/10.1016/0148-9062\(71\)90018-0](https://doi.org/10.1016/0148-9062(71)90018-0).
- Lak, M., Fatehi Marji, M., Yarahamdi Bafghi, A., Abdollahipour, A. (2019): ‘Discrete element modeling of explosion-induced fracture extension in jointed rock masses’, *Journal of Mining and Environment*, 10(1), 125–138. <https://doi.org/10.22044/jme.2018.7291.1579>.
- Lanari, M. and Fakhimi, A. (2014): DEM-SPH simulation of rock blasting. *Computational Geotechnique*, 158–164. <https://doi.org/10.1016/j.compgeo.2013.08.008>.
- Lanari, M. and Fakhimi, A. (2015): Numerical study of contributions of shock wave and gas penetration toward induced rock damage during blasting. *Computational Particle Mechanics*, 2, 197–208. <https://doi.org/10.1007/s40571-015-0053-8>.
- Liu, K., Hao, H. and Li, X. (2018): Numerical analysis of the stability of abandoned cavities in bench blasting. *International Journal of Rock Mechanics and Mining Sciences*, 9, 30–39. <https://doi.org/10.1016/j.ijrmms.2016.12.008>.
- Luccioni, B. et al. (2018): Experimental and numerical analysis of blast response of High Strength Fiber Reinforced Concrete slabs. *Engineering Structures*, 175, 11–22. <https://doi.org/10.1016/j.engstruct.2018.08.016>.
- Minchinton, A. and Lynch, P. (1996): Fragmentation and heave modeling using a coupled discrete element gas code. In: Mohanty, B. (ed.): *Rock fragmentation by blasting*. AA Balkema: Rotterdam, The Netherlands, 71–80, 472 p.
- Motoyama, Y., Mikame, S., Nojima, K., and Kawahara, M. (2014): Second-order adjoint equation method for parameter identification of rock based on blast waves in tunnel excavation. *Engineering Optimization*, 46(7), 939–963. <https://doi.org/10.1080/0305215X.2013.806917>.
- Ning, Y., Yang, J., Ma, G., and Chen, P. (2011): Modelling rock blasting considering explosion gas penetration using discontinuous deformation analysis. *Rock mechanics and rock engineering*, 44, 483–490. <https://doi.org/10.1007/s00603-010-0132-3>.
- Onederra, I. et al. (2013): Modeling blast induced damage from a fully coupled explosive charge. *International Journal of Rock Mechanics and Mining Sciences*, 58, 73–84. <https://doi.org/10.1016/j.ijrmms.2012.10.004>.
- Potyondy, D., Cundall, P. and Sarracino, R. (1996): Modeling of shock- and gas driven fractures induced by a blast using bonded assemblies of spherical particles. In: Mohanty, B. (ed.): *Rock fragmentation by blasting*. AA Balkema: Rotterdam, The Netherlands, 55–62, 472 p.
- Roy, P. P. (2005): Rock blasting: effects and operations. AA Balkema: Leiden, The Netherlands, 345 p.
- Rustan, A. (1998): Rock blasting terms and symbols: a dictionary of symbols and terminology in rock blasting and related areas like drilling. CRC Press, London, 204 p. <https://doi.org/10.1201/9781466571785>.
- Salamy, A.A. and Hammoud, I. (2023): Simulation of blast-induced rock tunnel damage using a 3D numerical model. *International Journal of Protective Structures*. <https://doi.org/10.1177/20414196231167596>.
- Sołtys, A., Twardosz, M. and Winzer, J. (2017): Control and documentation studies of the impact of blasting on buildings in the surroundings of open pit mines. *Journal of Sustainable Mining*, 16(4), 179–188. <https://doi.org/10.1016/j.jsm.2017.12.004>.
- Tiwari, R., Chakraborty, T., and Matsagar, V. (2016): Dynamic analysis of a twin tunnel in soil subjected to internal blast loading. *Indian Geotechnical Journal*, 46(4), 369–380. <https://doi.org/10.1007/s40098-016-0179-5>.
- Trigueros, E. et al. (2017): A methodology based on geomechanical and geophysical techniques to avoid ornamental stone damage caused by blast-induced ground vibrations. *International Journal of Rock Mechanics and Mining Sciences*, 93, 196–200. <https://doi.org/10.1016/j.ijrmms.2016.12.013>.
- Ulusay, R. (2014): The present and future of rock testing: highlighting the ISRM suggested methods. *The ISRM Suggested Methods for Rock Characterization, Testing and Monitoring: 2007-2014*, 1–22. [https://doi.org/10.1007/978-3-319-07713-0\\_1](https://doi.org/10.1007/978-3-319-07713-0_1).
- Wang, Z. et al. (2023): Numerical prediction of blast fragmentation of reinforced concrete slab using ALE-FEM-SPH coupling method. *Finite Elements in Analysis and Design*, 220, p. 103948. <https://doi.org/10.1016/J.FINEL.2023.103948>.
- Wang, Z., Yong-chi, L. and Wang, J. (2008): Numerical analysis of blast induced wave propagation and spalling damage in a rock plate. *International Journal of Rock Mechanics and Mining Sciences*, 45, 600–608. <https://doi.org/10.1016/j.ijrmms.2007.08.002>.
- Wei, X., Zhao, Z. and Gu, J. (2009): Numerical simulations of rock mass damage induced by underground explosion. *International Journal of Rock Mechanics and Mining Sciences*, 46, 1206–1213. <https://doi.org/10.1016/j.ijrmms.2009.02.007>.
- Yan, P., Zou, Y.J., Lu, W.B., Hu, Y.G., Leng, Z.D., Zhang, Y.Z., Liu, L., Hu, H.R., Chen, M., and Wang, G. H. (2016). Real-time assessment of blasting damage depth based on the induced vibration during excavation of a high rock slope.

- Geotechnical Testing Journal, 39(6), 991-1005. <https://doi.org/10.1520/GTJ20150187>.
- Yang, J., Lu, W., Chen, M., Yan, P., and Zhou, C. (2013): Microseism induced by transient release of in situ stress during deep rock mass excavation by blasting. *Rock Mechanics and Rock Engineering*, 46, 859-875. <https://doi.org/10.1007/s00603-012-0308-0>.
- Yang, J., Shi, C., Yang, W., Chen, X., and Zhang, Y. (2019): Numerical simulation of column charge explosive in rock masses with particle flow code. *Granular Matter*, 21(4), 96. <https://doi.org/10.1007/s10035-019-0950-2>.
- Yang, R., Ding, C., Yang, L., Lei, Z., Zhang, Z., & Wang, Y. (2018): Visualizing the blast-induced stress wave and blasting gas action effects using digital image correlation. *International Journal of Rock Mechanics and Mining Sciences*, 112, 47-54. <https://doi.org/10.1016/j.ijrmms.2018.10.007>.
- Zarate, F. et al. (2018): A coupled FEM-DEM procedure for predicting blasting operations in tunnels. *Underground Space*, 3(3), 310-316. <https://doi.org/10.1016/j.undsp.2018.09.002>.
- Zhu, Z., Mohanty, B. and Xie, H. (2007): Numerical investigation of blasting-induced crack initiation and propagation in rocks. *International Journal of Rock Mechanics and Mining Sciences*, 44, 600-608. <https://doi.org/10.1016/j.ijrmms.2006.09.002>.

## SAŽETAK

### Analiza utjecaja različitih energija eksplozije na razaranje stijena pomoću numeričkoga modeliranja

Širenje valova uzrokovanih eksplozijom izaziva vlačna i tlačna naprezanja u stijeni i utječe na njezino mehaničko i dinamičko ponašanje te na kraju dovodi do njezina razaranja. U tome procesu važna je pojava širenja pukotine te privlači pozornost raznih istraživača u novije vrijeme. Predviđanje geometrije loma u stijenskim materijalima, posebno u kontekstu porasta pukotina, složen je problem koji zahtijeva napredne tehnike modeliranja. U ovome istraživanju izbušena je minska bušotina u uzorku betona, a metodom diskretnih elemenata proučavana su četiri obilježja eksplozije. To su istovremeno modeliranje energije udara, refleksije i tlaka plina; istovremeno modeliranje energije udara i tlaka plina; istovremeno modeliranje energije udara i refleksije i samo modeliranje udarne energije. Iako homogenost umjetnih uzoraka poput betona neće točno oponašati uzorke kamena, saznanja iz ovoga istraživanja korisna su u okviru ograničenja koja imaju. Rezultati pokazuju da se najveća gustoća pukotina, odnosno najveća fragmentacija stijene događa kada su istovremeno prisutne sve tri vrste energije: udar, refleksija i tlak plina. Nadalje, rezultati pokazuju da model koji uključuje tlak plina i energiju udara pokazuje najveću fragmentaciju stijene, a slijedi ga model koji uzima u obzir samo energiju udara i refleksije. Model koji simulira udarnu energiju pokazuje najmanju fragmentaciju.

#### Ključne riječi:

udarni val, udarna energija, energija refleksije, tlak plina, numeričko modeliranje

## Author's contribution

**Seyed Mohammad Reza Sahlabadi (1)** (PhD candidate) carried out the numerical simulation and provided analyses, writing, presentation and interpretation of the results. **Kaveh Ahangari (2)** (Full Professor at the Faculty of Engineering) proposed the key ideas and contributed to the methodology, interpretation, and analyses of results. **Mosleh Eftekhari (3)** (Assistant Professor at the Faculty of Engineering) managed the whole process and supervised it from the beginning to the end.